

Gravitational waves from axisymmetrically oscillating neutron stars in general relativistic simulations

Masaru Shibata and Yu-ichirou Sekiguchi

Graduate School of Arts and Sciences, University of Tokyo, Tokyo, 153-8902, Japan

Abstract

Gravitational waves from oscillating neutron stars in axial symmetry are studied performing numerical simulations in full general relativity. Neutron stars are modeled by a polytropic equation of state for simplicity. A gauge-invariant wave extraction method as well as a quadrupole formula are adopted for computation of gravitational waves. It is found that the gauge-invariant variables systematically contain numerical errors generated near the outer boundaries in the present axisymmetric computation. We clarify their origin, and illustrate it possible to eliminate the dominant part of the systematic errors. The best corrected waveforms for oscillating and rotating stars currently contain errors of magnitude $\sim 10^{-3}$ in the local wave zone. Comparing the waveforms obtained by the gauge-invariant technique with those by the quadrupole formula, it is shown that the quadrupole formula yields approximate gravitational waveforms besides a systematic underestimation of the amplitude of $O(M/R)$ where M and R denote the mass and the radius of neutron stars. However, the wave phase and modulation of the amplitude can be computed accurately. This indicates that the quadrupole formula is a useful tool for studying gravitational waves from rotating stellar core collapse to a neutron star in fully general relativistic simulations. Properties of the gravitational waveforms from the oscillating and rigidly rotating neutron

stars are also addressed paying attention to the oscillation associated with fundamental modes.

04.25.Dm, 04.30.-w, 04.40.Dg

I. INTRODUCTION

One of the most important roles of numerical simulations in general relativity is to predict gravitational waveforms emitted by general relativistic and dynamical astrophysical phenomena. Rotating stellar core collapse and nonspherical oscillation of neutron stars are among the possible sources of gravitational waves. Therefore, fully general relativistic numerical simulation for them is an important subject in this field [1].

To date, there has been no systematic work for computation of gravitational waves from rotating stellar core collapse to a neutron star in fully general relativistic simulation (but see [2]). The gravitational waveforms have been computed only in the Newtonian gravity [3–9] or in an approximate general relativistic gravity [1] using the so-called conformal flatness approximation (or Isenberg-Wilson-Mathews approximation). As demonstrated in [1], general relativistic effects modify the evolution of the collapse and emitted gravitational waveforms significantly. Thus, the simulation in full general relativity appears to be the best approach for accurate computation of gravitational waves.

In the case that the progenitor of the core collapse is not very rapidly rotating, nonaxisymmetric instabilities do not set in and, hence, the collapse will proceed in an axisymmetric manner. In such a collapse, the amplitude of gravitational waves measured in a local wave zone at $r \approx \lambda$ where λ denotes the gravitational wave length will be smaller, by two or three orders of magnitude, than that in highly nonaxisymmetric phenomena such as mergers of binary neutron stars and black holes. The amplitude of gravitational waves from an oscillating neutron star is also likely to be small due to its small nonspherical deformation. Technically, it is not easy to extract gravitational waves of small amplitude from metric computed in numerical simulations, in which a numerical noise is in general contained. The numerical noise is generated due to the following reasons:

Gravitational waves are usually extracted from the metric in the wave zone in general relativistic simulations. Although they should be extracted at the null infinity, the outer boundaries of computational domain are located at a finite radius whenever the 3+1 for-

malisms are adopted. Thus, the outer boundary conditions are imposed at finite radii and in general they are approximate conditions. As a result, a small numerical error may be excited around the outer boundaries. Here, the possible candidates of the numerical error are unphysical nonwave modes, spurious gauge modes, back reflections at the outer boundaries, and roundoff errors.

In this paper, we study gravitational waves from oscillating neutron stars in axial symmetry. Neutron stars in equilibrium are simply modeled by $n = 1$ polytropes. Oscillations of neutron stars are followed by axisymmetric numerical simulations in full general relativity. Gravitational waves are extracted using a gauge-invariant wave extraction technique. The gauge-invariant variables are not contaminated by gauge modes and, hence, we can focus on other error sources using this variables. We also adopt a quadrupole formula for approximately computing gravitational waveforms to clarify its validity.

This work was planned from the following four motivations. The first one is to specify the error sources contained in the gauge-invariant variables extracted in the local wave zone. As mentioned above, they could be contaminated by nonwave components and numerical errors. In particular, it is important to specify systematic error components contained in the gauge-invariant variables since as indicated in Sec. IV, the systematic errors may be eliminated at least partly if their origin is clarified.

The second motivation is to understand how large computational domains are needed to extract gravitational waveforms within $\sim 10\%$ error. Since the gauge-invariant variables are extracted at finite radii, gravitational waveforms (in particular the amplitude) are slightly different from the asymptotic ones. It is important to clarify how magnitude of the error depends on the radius at which we impose the outer boundary conditions and on the radius at which we extract gravitational waves. A similar study was carried out about 15 years ago by Abrahams and Evans [10]. However, they were interested only in specific gauge conditions which were often used in axisymmetric numerical simulations in general relativity at that time. Moreover, the simulations were carried out only for non-rotating stars. In this paper, we adopt a different gauge condition often used nowadays in three-dimensional simulations,

and report numerical results both for nonrotating and rotating stars.

The third motivation, in which we are most interested in the present study, is to investigate validity of a quadrupole formula in fully general relativistic simulations. For computation of gravitational waves generated by oscillations of gravitational field such as quasinormal mode ringings of black holes, quadrupole formulas cannot work. However, in rotating stellar core collapse to a neutron star and in oscillating neutron stars in which gravitational waves are generated mainly by matter motions, quadrupole formulas may be able to yield an accurate waveform. This method can be applied much more easily than geometrical methods in which gravitational waves are extracted from metric in the wave zone. Thus, a quadrupole formula which can yield high-quality approximate waveforms will be a robust method for computing gravitational waves of small amplitude from a noisy numerical data set. Note that a similar work has been already done by Siebel et al. [11,2] in a null-cone formulation. We here carry out the similar study for a 3+1 approach.

The last motivation is to understand the properties of oscillations of rotating neutron stars. During rotating stellar core collapse, gravitational waves associated with oscillations of a formed protoneutron star are likely to be emitted (see, e.g., [1]). From the study for oscillating and rotating neutron stars, we will be able to understand what oscillation modes are relevant for the emission of gravitational waves during core collapses. We here pay attention to two fundamental oscillation modes (quasiradial and quadrupole p modes of no node for the density perturbation) which are candidates for the dominant modes in the oscillating and rotating stars formed after the collapse.

This paper is organized as follows. In Sec. II, our numerical implementations for axisymmetric general relativistic simulation are briefly reviewed. In Sec. III, the gauge-invariant wave extraction technique and the quadrupole formula adopted in the present work are described. Sec. IV presents numerical results of gravitational waveforms emitted from oscillating neutron stars. The simulations were performed both for nonrotating and rotating neutron stars using an axisymmetric code recently developed [12]. Sec. IV is devoted to a summary. Throughout this paper, we adopt the geometrical units in which $G = c = 1$ where

G and c are the gravitational constant and the speed of light, respectively.

II. NUMERICAL IMPLEMENTATION

A. Summary of formulation

We performed fully general relativistic simulations in axial symmetry using the same formulation as that in [12], to which the readers may refer for details and basic equations. The fundamental variables for hydrodynamics are:

ρ : rest mass density,

ε : specific internal energy,

P : pressure,

u^μ : four velocity,

$$v^i = \frac{dx^i}{dt} = \frac{u^i}{u^t}, \quad (1)$$

where subscripts i, j, k, \dots denote x, y , and z , and μ the spacetime components. In addition, we define a weighted density $\rho_*(= \rho\alpha u^t e^{6\phi})$ and a weighted four-velocity $\hat{u}_i(= (1+\varepsilon+P/\rho)u_i)$. From these variables, the total baryon rest-mass and angular momentum of system, which are conserved quantities in axisymmetric spacetimes, can be defined as

$$M_* = \int d^3x \rho_*, \quad (2)$$

$$J = \int d^3x \rho_* \hat{u}_\varphi. \quad (3)$$

General relativistic hydrodynamic equations are solved using a so-called high-resolution shock-capturing scheme [14,15,12] in cylindrical coordinates (or on $y = 0$ plane in Cartesian coordinates).

The fundamental variables for geometry are:

α : lapse function,

β^k : shift vector,

γ_{ij} : metric in 3D spatial hypersurface,

$$\gamma = e^{12\phi} = \det(\gamma_{ij}),$$

$$\tilde{\gamma}_{ij} = e^{-4\phi} \gamma_{ij},$$

K_{ij} : extrinsic curvature. (4)

We evolve $\tilde{\gamma}_{ij}$, ϕ , $\tilde{A}_{ij} \equiv e^{-4\phi}(K_{ij} - \gamma_{ij}K_k^k)$, and the trace of the extrinsic curvature K_k^k together with three auxiliary functions $F_i \equiv \delta^{jk}\partial_j\tilde{\gamma}_{ik}$ with an unconstrained free evolution code as done in [16,17,19,20,12].

The Einstein equations are solved in the Cartesian coordinates. To impose axisymmetric boundary conditions, the Cartoon method is adopted [13]: Assuming a reflection symmetry with respect to the equatorial plane, we perform simulations using a fixed uniform grid with the grid size $N \times 3 \times N$ for (x, y, z) which covers a computational domain as $0 \leq x \leq L$, $0 \leq z \leq L$, and $-\Delta \leq y \leq \Delta$. Here, N and L are constants and $\Delta = L/N$. For $y = \pm\Delta$, the axisymmetric boundary conditions are imposed using data sets on the $y = 0$ plane.

The slicing and spatial gauge conditions adopted in this paper are basically the same as those in [16–19]; i.e., we impose an “approximately” maximal slice condition ($K_k^k \approx 0$) and an “approximately” minimal distortion gauge condition [$\tilde{D}_i(\partial_t\tilde{\gamma}^{ij}) \approx 0$ where \tilde{D}_i is the covariant derivative with respect to $\tilde{\gamma}_{ij}$] [16,17,19]. In the approximately minimal distortion gauge condition, F_i is zero in the linear order in $h_{ij}(\equiv \tilde{\gamma}_{ij} - \delta_{ij})$ if $F_i = 0$ initially. Thus, in the wave zone, h_{ij} approximately satisfies a transverse condition $h_{ij,j} = 0$.

We also performed a few simulations using a dynamical gauge condition [21] in which we solve

$$\partial_t\beta^k = \tilde{\gamma}^{kl}(F_l + \Delta t\partial_t F_l), \tag{5}$$

where Δt denotes a timestep in a numerical computation. We have found that the magnitude of the numerical error depends weakly on the spatial gauge condition, but gravitational waveforms and qualitative nature of the numerical error do not. Thus, in this paper, we present the results obtained in the approximately minimal distortion gauge condition.

During numerical simulations, violations of the Hamiltonian constraint and conservation of mass and angular momentum are monitored as code checks. Numerical results for several test calculations, including stability and collapse of nonrotating and rotating neutron stars, have been described in [12]. Several convergence tests have been also presented in [12].

B. Outer boundary conditions

Outer boundary conditions for geometric variables have been modified from previous ones [16–19]. We impose a boundary condition for ϕ as

$$\phi = \frac{M}{2r} + O(r^{-2}), \quad (6)$$

where M denotes the ADM mass of a system computed at $t = 0$. We note that M is an approximately conserved quantity in axial symmetry, since only a small amount of gravitational waves are emitted in axisymmetric oscillations.

For $h_{ij}(= \tilde{\gamma}_{ij} - \delta_{ij})$, we first carry out a coordinate transformation from the Cartesian coordinates to spherical polar coordinates (r, θ, φ) with the flat metric, η_{ab} [the subscripts a and b denote components of the spherical polar coordinates (r, θ, φ)], and then impose outgoing-wave outer boundary conditions of the form

$$\begin{aligned} h_{\hat{r}\hat{r}}r^3 &= f_1(t-r), \\ h_{\hat{r}\hat{\theta}}r^2 &= f_2(t-r), \\ h_{\hat{r}\hat{\varphi}}r^2 &= f_3(t-r), \\ h_{\hat{\theta}\hat{\theta}}r &= f_4(t-r), \\ h_{\hat{\theta}\hat{\varphi}}r &= f_5(t-r), \\ h_{\hat{\varphi}\hat{\varphi}}r &= f_6(t-r), \end{aligned} \quad (7)$$

where $h_{\hat{a}\hat{b}}$ denotes a tetrad component and f_i ($i = 1 \sim 6$) denote functions: Since $f_i(t-r) = f_i[t - \Delta t - (r - \Delta t)]$, the value of $f_i(t-r)$ at the outer boundaries should be equal to that at a time $t - \Delta t$ and at a radius $r - \Delta t$ which is determined using the values of 8

nearby grid points at a previous timestep [20]. These sets of the outer boundary conditions are well-suited for a solution of the linearized Einstein equation in the transverse-traceless gauge condition for h_{ab} if they are imposed in a distant wave zone [24]. In the local wave zone, however, equations (7) are approximate boundary conditions since higher order terms of $1/r$ are neglected. Therefore, numerical errors and unphysical solutions may be generated around the outer boundaries. In addition, h_{ij} should physically contain nonwave modes (such as stationary multipole modes) which do not obey the boundary conditions (7). Since no attention is paid to such modes in imposing the condition (7), additional numerical errors may be excited.

In the case of the approximately minimal distortion gauge, we adopt the same boundary conditions for F_i , K , and \tilde{A}_{ij} as those used in previous papers [16,17]: i.e., $F_i = K = 0$, and an outgoing-wave boundary condition is imposed for \tilde{A}_{ij} . In the dynamical gauge condition, an outgoing-wave boundary condition is imposed for F_i , because it obeys a hyperbolic-type equation.

III. WAVE EXTRACTION METHODS

A. Gauge-invariant technique

Gravitational waves are extracted in terms of a gauge-invariant technique [22,23]. In this method, the fully nonlinear 3-metric γ_{ab} in spherical polar coordinates is split as $\eta_{ab} + \xi_{ab}$, where ξ_{ab} is regarded as the perturbation on the flat background. In axial symmetry, ξ_{ab} can be decomposed as $\sum_l \zeta_{ab}^l$, where ζ_{ab}^l is given by

$$\zeta_{ab}^l = \begin{pmatrix} H_{2l}Y_{l0} & h_{1l}Y_{l0,\theta} & 0 \\ * & r^2(K_l Y_{l0} + G_l W_{l0}) & 0 \\ * & * & r^2 \sin^2 \theta (K_l Y_{l0} - G_l W_{l0}) \end{pmatrix}$$

$$+ \begin{pmatrix} 0 & 0 & C_l \partial_\theta Y_{l0} \sin \theta \\ * & 0 & -r^2 D_l W_{l0} \sin \theta \\ * & * & 0 \end{pmatrix}. \quad (8)$$

Here, * denotes the symmetric components. The first term in Eq. (8) corresponds to even parity (polar) perturbations and the second one to odd parity (axial) perturbations. The quantities H_{2l} , h_{1l} , K_l , G_l , C_l , and D_l are functions of r and t , and are calculated by performing integrations over a two-sphere of a given radius. Y_{l0} is the spherical harmonic function, and W_{l0} is defined as

$$W_{l0} \equiv [(\partial_\theta)^2 - \cot \theta \partial_\theta] Y_{l0}. \quad (9)$$

The gauge-invariant variables of even and odd parities are then defined as [22,23]

$$R_l^E(t, r) \equiv \sqrt{\frac{2(l-2)!}{(l+2)!}} \{2k_{2l} + l(l+1)k_{1l}\}, \quad (10)$$

$$R_l^O(t, r) \equiv \sqrt{\frac{2(l+2)!}{(l-2)!}} \left(\frac{C_l}{r} + r \partial_r D_l \right), \quad (11)$$

where

$$k_{1l} \equiv K_l + l(l+1)G_l + 2r \partial_r G_l - 2 \frac{h_{1l}}{r}, \quad (12)$$

$$k_{2l} \equiv H_{2l} - \frac{\partial}{\partial r} [r \{K_l + l(l+1)G_l\}]. \quad (13)$$

Luminosity of gravitational waves is computed from

$$\frac{dE}{dt} = \frac{r^2}{32\pi} \sum_l [|\partial_t R_l^E|^2 + |\partial_t R_l^O|^2]. \quad (14)$$

The time derivative of the gauge-invariant quantities in Eq. (14) is taken by a finite-differencing. Hereafter, we focus only on the even-parity mode with $l = 2$ because for the oscillations considered in this paper, its amplitude is much larger than that of other modes.

In an appropriate radiation gauge, +-mode of gravitational waves is extracted from the asymptotic behavior of the following quantity at $r \rightarrow \infty$;

$$h_+ \equiv \frac{1}{2r^2} \left(\gamma_{\theta\theta} - \frac{\gamma_{\varphi\varphi}}{\sin^2 \theta} \right). \quad (15)$$

For $l = 2$, h_+ can be written as

$$h_+ = \frac{A_2(t)}{r} \sin^2 \theta, \quad (16)$$

where $A_2(t)$ denotes a function of time. Using A_2 , the asymptotic behavior of R_2^E is written as

$$R_2^E \rightarrow \sqrt{\frac{64\pi}{15}} \frac{A_2}{r}. \quad (17)$$

B. Quadrupole formula

In quadrupole formulas, gravitational waves are computed from

$$h_{ij} = P_i^k P_j^l \left(\frac{2}{r} \frac{d^2 I_{kl}}{dt^2} \right), \quad (18)$$

where I_{ij} and $P_i^j = \delta_{ij} - n_i n_j$ ($n_i = x^i/r$) denote a tracefree quadrupole moment and a projection tensor. From this expression, +-mode of gravitational waves with $l = 2$ in axial symmetry is written as

$$h_+^{\text{quad}} = \frac{\ddot{I}_{xx}(t_{\text{ret}}) - \ddot{I}_{zz}(t_{\text{ret}})}{r} \sin^2 \theta, \quad (19)$$

where I_{ij} denotes an appropriately defined quadrupole moment, and \ddot{I}_{ij} its second time derivative. Equation (19) implies that in quadrupole formulas, $A_2(t) = \ddot{I}_{xx}(t_{\text{ret}}) - \ddot{I}_{zz}(t_{\text{ret}})$.

t_{ret} is a retarded time which is approximately defined by

$$t_{\text{ret}} = t - r_{\text{circ}} - 2M \ln \left(\frac{r_{\text{circ}}}{2M} - 1 \right), \quad (20)$$

where $r_{\text{circ}} = r(1 + M/2r)^2 \gg M$. Equation (20) is the valid expression only for the Schwarzschild spacetime. In axisymmetric spacetimes, the retarded time should depend on the direction of wave propagation. However, the magnitude of the difference between Eq.

(20) and the exact one would be of $O(M)$ and, hence, much smaller than the typical wave length.

In fully general relativistic and dynamical spacetimes, there is no unique definition for the quadrupole moment and, hence, for \ddot{I}_{ij} . Here, we choose for simplicity

$$I_{ij} = \int \rho_* x^i x^j d^3x. \quad (21)$$

Then, using the continuity equation of the form

$$\partial_t \rho_* + \partial_i (\rho_* v^i) = 0, \quad (22)$$

we can compute the first time derivative as

$$\dot{I}_{ij} = \int \rho_* (v^i x^j + x^i v^j) d^3x. \quad (23)$$

To compute \ddot{I}_{ij} , we carried out a finite differencing of the numerical result for \dot{I}_{ij} .

Since the quadrupole moment I_{ij} is not defined uniquely in the dynamical spacetime in general relativity, gravitational waveforms computed by quadrupole formulas depend on the form of I_{ij} . In addition, they depend on the gauge conditions, since a physical point which coordinates x^i and t denote (and, as a result, the magnitude of I_{ij} and \ddot{I}_{ij}) is not identical in two different gauge conditions. Even if an identical definition of the quadrupole formula is employed, waveforms do not in general agree when different gauge conditions are adopted. Therefore, we should keep in mind that the waveforms computed from Eq. (19) are special ones obtained in specific choices of I_{ij} and the gauge condition. All these facts imply that to know the validity of the quadrupole formula which one chooses, comparison between the waveforms by the quadrupole formula with those extracted from metric should be made.

IV. NUMERICAL RESULTS

A. Setting

The simulations were carried out along the following procedure: (1) neutron stars in equilibrium were prepared, (2) a perturbation to the equilibria was added, (3) the constraint

conditions were re-imposed by solving the constraint equations for the perturbed state, and then (4) we started the time evolution.

To model neutron stars in equilibrium, we simply adopt the polytropic equation of state as

$$P = K\rho^{1+\frac{1}{n}}, \quad (24)$$

where K is the polytropic constant and n the polytropic index. For the evolution of the neutron stars, we adopt a Γ -law equation of state in the form

$$P = (\Gamma - 1)\rho\varepsilon, \quad (25)$$

where $\Gamma = 1 + 1/n$. We set $n = 1$ ($\Gamma = 2$) as a reasonable qualitative approximation to cold, nuclear equation of state. With these equations of state, realistic neutron stars may not be modeled precisely. However, in the current situation that no one know a real equation of state of neutron stars exactly, modeling neutron stars with a simple equation of state is an adequate and popular strategy.

In the present choice of the equation of state, physical units enter the problem only through the polytropic constant K , which can be chosen arbitrarily or else completely scaled out of the problem. For $n = 1$, $K^{1/2}$ has units of length, time, and mass, and K^{-1} units of density in the geometrical units. Using this property, we rescale all the quantities to be nondimensional and show only the nondimensional quantities.

One often prefers to use particular dimensional units even in the polytropic equation of state. For example, in [15], the authors fix the value of K as 1.455×10^5 cgs. For the sake of comparison with the previous paper, we convert non-dimensional quantities to dimensional ones with the polytropic constant $K = 1.455 \times 10^5$ cgs. In this special value, the mass, the density, and the time in the dimensional units are written as

$$M_{\text{dim}} = 1.80M_{\odot} \left(\frac{K}{1.455 \times 10^5 \text{ cgs}} \right)^{1/2} \left(\frac{M}{0.180} \right), \quad (26)$$

$$\rho_{\text{dim}} = 1.86 \times 10^{15} \text{ g/cm}^3 \left(\frac{K}{1.455 \times 10^5 \text{ cgs}} \right)^{-1} \left(\frac{\rho}{0.300} \right), \quad (27)$$

$$T_{\text{dim}} = 4.93 \text{ msec} \left(\frac{K}{1.455 \times 10^5 \text{ cgs}} \right)^{1/2} \left(\frac{T}{100} \right). \quad (28)$$

	ρ_c	M_*	M	M/R	J/M^2	$P_{\text{osc}}/(2\pi R^{3/2} M^{-1/2})$
S1	0.127	0.150	0.140	0.146	0	0.84
S2	0.191	0.170	0.156	0.178	0	0.84
S3	0.255	0.178	0.162	0.200	0	0.85
R1	0.103	0.169	0.158	0.111(0.181)	0.667	0.48
R2	0.118	0.178	0.165	0.120(0.194)	0.648	0.48
R3	0.136	0.186	0.172	0.129(0.207)	0.630	0.50

TABLE I. Central density ρ_c , baryon rest-mass M_* , ADM mass M , compactness M/R , angular momentum J in units of M^2 , and numerical results for fundamental radial oscillation period with $l = 2$ in units of $2\pi R^{3/2}/M^{1/2}$ of neutron stars that we pick up in this paper. Here, R denotes the circumference radius at the equatorial surface. For the rotating stars, the compactness measured by the polar radius is also listed in the bracket. All the quantities are shown in units of $c = G = K = 1$.

We adopted six models of neutron stars referred to as S1–S3 and R1–R3 in this numerical experiment. Models S1–S3 are spherical stars and R1–R3 are rigidly and rapidly rotating stars whose angular velocities at the equatorial surface are approximately equal to the Keplerian angular velocity (i.e., at mass-shedding limits). By exploring rotating stars at the mass-shedding limits, the effects of rotation on rigidly rotating neutron stars are clarified most efficiently.

The maximum gravitational masses of spherical stars and rigidly rotating stars with $n = 1$ ($\Gamma = 2$) are $\approx 0.164K^{1/2}$ and $\approx 0.188K^{1/2}$, respectively [25]. Thus, the models adopted here are sufficiently general relativistic in the sense that their masses are close to the maximum values. In Table I, characteristic quantities for models S1–S3 and R1–R3 are listed in the nondimensional units (in the units with $c = G = K = 1$).

To induce nonspherical stellar oscillations to nonrotating stars, we superimposed a velocity perturbation as

$$\delta u_{\varpi} = -V\varpi \quad \text{and} \quad \delta u_z = Vz, \quad (29)$$

where δu_{ϖ} and δu_z denote the four-velocity of cylindrical ($\varpi = \sqrt{x^2 + y^2}$) and z components. V is a constant and put as $V = 0.1/\varpi_e$ where ϖ_e denotes the coordinate radius at the equator: i.e., at the equatorial surface, the velocity is $\approx 10\%$ of the light speed.

For the rotating stars, two types of the perturbations are adopted. One is a velocity perturbation given by

$$\delta u_{\varpi} = -\frac{V}{2}\varpi \quad \text{and} \quad \delta u_z = Vz, \quad (30)$$

with $V = 0.3/\varpi_e$. The other is a pressure perturbation in which we simply reduced the pressure uniformly by changing the polytropic constant from the equilibrium value to a smaller one. In this case, a quasiradial oscillation is induced. Since the rotating star is nonspherical, gravitational waves are emitted even in this setting.

The simulations were performed changing grid spacing and location of outer boundaries. As found in [12], the numerical results are sufficiently convergent if the stellar radius is covered by more than 30 grid points. Taking into account this fact, the grid spacing is fixed in the simulations of this paper as follows: For nonrotating stars, we chose it as $\varpi_e/40$, and for rotating stars, $\varpi_e/60$: Since the axial ratio of the rotating stars at the mass-shedding limit is ≈ 0.59 , the polar axis is initially covered by about 36 grid points with this setting.

On the other hand, the location of the outer boundaries was changed varying N from 480 to 720. We typically choose $N = 720$, since with this number, L is larger than a characteristic gravitational wave length λ and, thus, the outer boundaries are located in a local wave zone. Since $L > \lambda$, we expect that the amplitude of gravitational waves could be calculated within $\sim 10\%$ error.

Table II describes the values of L and the location L_e at which the gauge-invariant variables are extracted. Typically, L_e is chosen to be $\sim 0.9L$. Note that varying L_e from $L/2$ to $0.95L$, it is found that the amplitude of gravitational waves depends very weakly on the location of L_e [see Figs. 1(b) and 2(b)] for a fixed value of L .

Nonrotational	L/M for $N = 480, 600, 720$	L_e/M for $N = 480, 600, 720$	λ/M
S1	64.4, 80.5, 96.6	53.5, 66.9, 80.3	94.8
S2	57.5, 71.9, 86.3	47.8, 59.8, 71.8	70.5
S3	55.4, 69.3, 83.2	46.1, 57.6, 69.2	60.5

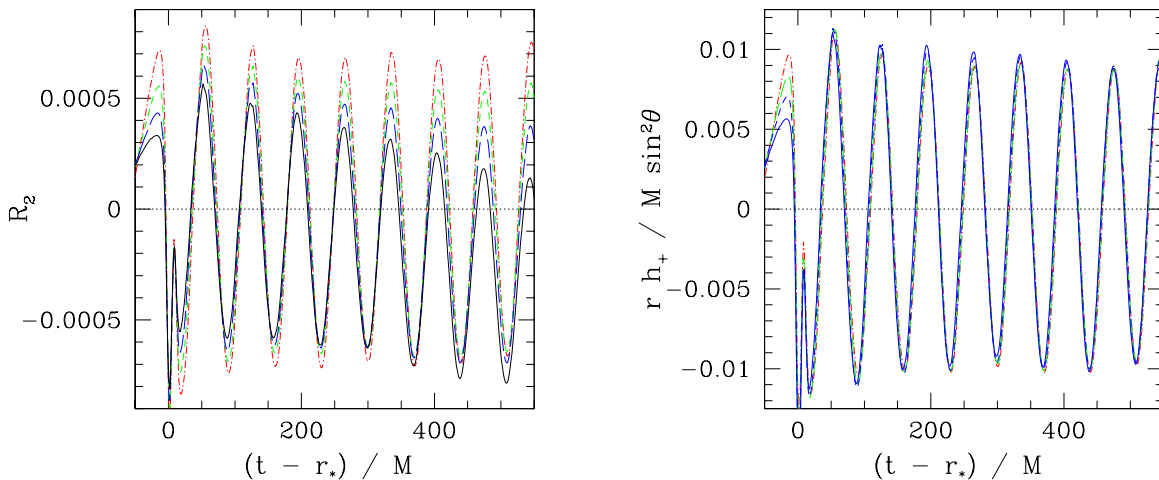
Rotational	L/M for $N = 480, 720$	L_e/M for $N = 480, 720$	λ/M
R1	63.3, 94.9	57.9, 86.9	80.8
R2	58.0, 87.0	53.1, 79.6	73.3
R3	53.2, 79.8	48.7, 73.0	66.5

TABLE II. Values of L and L_e in units of M for various values of N . For comparison, we show a gravitational wave length for the fundamental quadrupole ($l = 2$) mode derived from numerical results.

B. Systematic numerical errors

Since the outer boundaries are located in the local wave zone and, hence, the boundary conditions which are appropriate only for the distant wave zone are not precise ones, systematic numerical errors are generated around the outer boundaries. As a consequence, gravitational waveforms (gauge-invariant variables) are contaminated by numerical errors. To accurately extract gravitational waves, we need to eliminate the errors from raw data sets of the gauge-invariant variables.

First, we summarize the behavior of the numerical errors. In Figs. 1(a) and 2(a), we display time evolution of raw data sets of the gauge-invariant variables extracted at several radii for models S2 and R2 with $N = 720$. The gauge-invariant variables are composed mainly of three components; (i) a pure wave component which denotes gravitational waves, (ii) a constant component, and (iii) a secular drift component whose magnitude increases with time and is larger for the larger value of radius. To obtain clear gravitational waveforms,



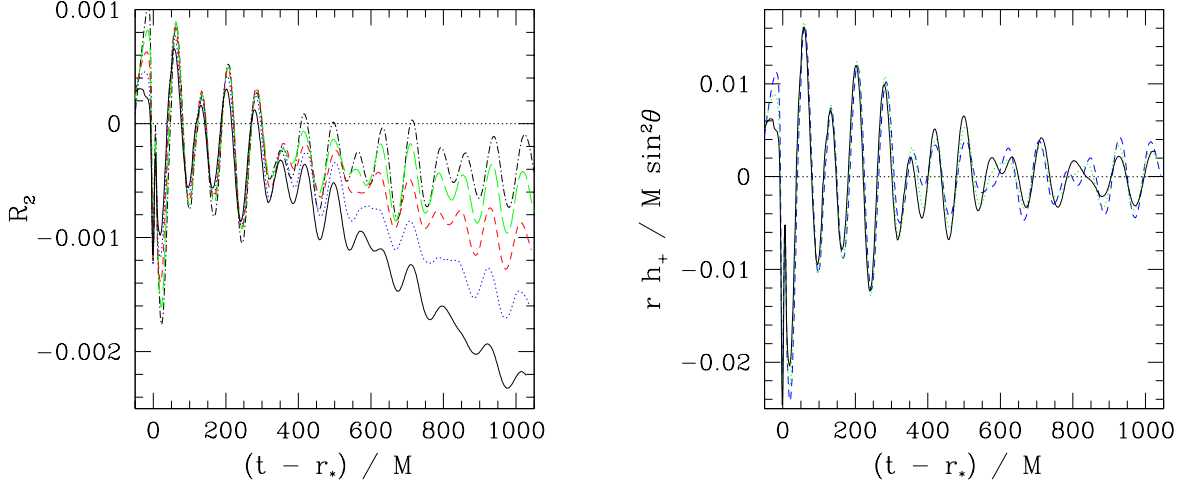
(a) (b)
 FIG. 1. (a) Gauge-invariant variables with $l = 2$ in units of M for oscillation of a nonrotating neutron star S2 extracted at $r/M = 50.2$ (dotted-dashed curve), 57.4 (dashed curve), 64.6 (long-dashed curve), and 71.8 (solid curve). (b) gravitational waveforms after systematic numerical errors are subtracted. In the simulation, $N = 720$.

it is necessary to eliminate the components (ii) and (iii).

The presence of the component (ii) is in part due to the fact that the gauge-invariant variables are computed at finite radii. They are composed not only of gravitational waves but also of a quasistationary component which falls off as r^{-n} for $n \geq 2$. In particular, rapidly rotating stars are of spheroidal shape and, hence, they yield quasistationary quadrupole and higher multipole moments which slowly vary throughout the simulation. As Fig. 2(a) shows (see for $t - r_* < 0$), this component is smaller for the larger value of extracted radius because it falls off as r^{-n} with $n \geq 2$.

A part of the component (ii) and the component (iii) are numerical errors associated with an approximate treatment of the outer boundary conditions. In the following, we explain the origin of it in detail.

In the wave zone, the magnitude of h_{ij} is small and, hence, it approximately obeys a linearized Einstein equation. In the formalism which we currently use [19], the linearized equation for h_{ij} is of the form



(a) (b)
 FIG. 2. (a) Gauge-invariant variables with $l = 2$ in units of M for oscillation of a rotating neutron star R2 extracted at $r/M = 50.7$ (dotted-dashed curve), 57.9 (long-dashed curve), 65.2 (dashed curve), 72.4 (dotted curve), and 79.6 (solid curve). (b) gravitational waveforms after systematic numerical errors are subtracted at $r/M = 65.2$ (dashed curve), 72.4 (dotted curve), and 79.6 (solid curve). The simulation was performed with $N = 720$.

$$\ddot{h}_{ij} = \Delta_f h_{ij} + S_{ij}^h, \quad (31)$$

where Δ_f denotes the flat Laplacian and S_{ij}^h is composed of spatial derivatives of $a \equiv \alpha - 1$, $\dot{\beta}^i$, $p \equiv e^\phi - 1$, and F_k as

$$\begin{aligned} S_{ij}^h = & (4p + 2a)_{|ij} - \frac{1}{3} \eta_{ij} \Delta_f (4p + 2a) \\ & + \eta_{ik} \dot{\beta}^k_{|j} + \eta_{jk} \dot{\beta}^k_{|i} - \frac{2}{3} \eta_{ij} \dot{\beta}^k_{|k} - \left(F_{i|j} + F_{j|i} - \frac{2}{3} \eta_{ij} \eta^{kl} F_{k|l} \right). \end{aligned} \quad (32)$$

Here, $|i$ denotes the covariant derivative with respect to the flat metric η_{jk} .

Because of the functional form of S_{ij}^h , the solution of h_{ij} may be written as

$$h_{ij} = h_{ij}^{\text{GW}} + \xi_{i|j} + \xi_{j|i} - \frac{2}{3} \eta_{ij} \xi^k_{|k}, \quad (33)$$

where h_{ij}^{GW} and ξ_k obey the following equations:

$$\ddot{h}_{ij}^{\text{GW}} = \Delta_f h_{ij}^{\text{GW}}, \quad (34)$$

$$\ddot{\xi}_k = \Delta_f \xi_k + \dot{\beta}_k + (2p + a)_{|k} - F_k. \quad (35)$$

Since the inhomogeneous solution of h_{ij} , which is associated with S_{ij}^h , is written by a gauge variable ξ_k , S_{ij}^h does not contribute the gauge-invariant variable*.

Gravitational waves may be extracted from G_2 , which is calculated by

$$G_2 = \frac{1}{48} \oint (h_{\hat{\theta}\hat{\theta}} - h_{\hat{\varphi}\hat{\varphi}}) W_{20} dS. \quad (37)$$

This variable can be regarded as gravitational waves in gauge conditions in which $\xi_k = 0$ (e.g., in the harmonic gauge condition). However, in the present case, ξ_k is not guaranteed to be vanishing and the effects of ξ_k are contained in G_2 . Consequently, the waveforms may be deformed by unphysical modulations and secular drifts due to the presence of ξ^k . This illustrates that the gauge-invariant technique plays an important role for extraction of gravitational waves in general gauge conditions.

General forms of outgoing-wave solutions of Eq. (34) for h_{ij}^{GW} have been derived by Teukolsky [24] and Nakamura [27]. However, numerically, such solutions can be exactly computed only when (A) a strict outgoing-wave boundary condition well-suited in a local wave zone is imposed and (B) the transverse condition is guaranteed. In the present numerical simulations, these conditions are not satisfied strictly. Therefore, unphysical modes as well as numerical errors contaminate numerical solutions of h_{ij}^{GW} .

One of the candidates for the dominant unphysical modes is a solution for the equations $\Delta_f h_{ij}^{\text{GW}} = 0$ and $\ddot{h}_{ij}^{\text{GW}} = 0$. From the relation $\ddot{h}_{ij}^{\text{GW}} = 0$, h_{ij}^{GW} is written as $H_{ij}^0(x) + H_{ij}^1(x)t$

*The gauge-invariant variables are computed from $\gamma_{ij} - \eta_{ij} \equiv H_{ij}$. In the linear order, $H_{ij} = h_{ij} + 4p\eta_{ij}$. The linearized Einstein equation for H_{ij} in our formulation [16,19] is

$$\ddot{H}_{ij} = \Delta_f H_{ij} + (4p + 2a)_{|ij} + \eta_{ik} \dot{\beta}_{|j}^k + \eta_{jk} \dot{\beta}_{|i}^k - (F_{ij} + F_{j|i}) - \frac{2}{3} \eta_{ij} (8\Delta_f p - \eta^{kl} F_{k|l}). \quad (36)$$

If the Hamiltonian constraint in the linear level is satisfied, $8\Delta_f p - \eta^{kl} F_{k|l} = 0$. Then, the solution of H_{ij} is $\bar{h}_{ij} + \xi_{i|j} + \xi_{j|i}$, and consequently, the gauge-invariant variables do not contain ξ_i . However, if the Hamiltonian constraint is violated, the effects of ξ_i is contained in the gauge-invariant variables. In the present work, we found that its effect is small, and hence we ignore it.

where H_{ij}^0 and H_{ij}^1 satisfy the Laplace equation. Note that H_{ij}^n ($n = 0$ and 1) do not satisfy the transverse-traceless condition in general. By performing a spherical harmonic decomposition of h_{ij} in the spherical polar coordinates (see Appendix A), we find the asymptotic behavior of the solutions of l -th moment for $r \gg M$ as

$$H_{ij}^n \rightarrow r^{l\pm 2}, r^l, r^{-l\pm 1}, \text{ and } r^{-l-3}. \quad (38)$$

The solutions of r^{l-2} and r^{-l-3} can be written in the form $V_{i|j} + V_{j|i}$ where V_i denotes a vector. These components are eliminated from the gauge-invariant variables. However, other solutions cannot be written in terms of V_i . Thus, four of six solutions may be contained in the gauge-invariant variables as unphysical modes. Properties of the unphysical solutions are summarized as follows: (a) they may increase linearly with time and (b) they may be larger for larger extracted radii because of the presence of the modes proportional to r^{l+2} and r^l . These properties agree with the numerical results shown in Figs. 1(a) and 2(a).

Besides the global numerical errors described above, unphysical local waves of the form $f(t \pm r)$ may be contained in h_{ij}^{GW} . However, this is not a systematic error and, hence, it is not possible to eliminate systematically. Fortunately, the magnitude of such components is not as large as that of the systematic errors (see below).

The systematic non-wave components may be fitted using a function of the form $C = C_0(r) + C_1(r)t$. Thus, we determine C_0 and C_1 and then subtract C from the gauge-invariant variables. As mentioned above, $C_0(r)$ arises both from a nonwave component associated with the stationary quadrupole moment and from the unphysical modes associated with H_{ij}^n . $C_1(r)t$ arises from the unphysical modes associated with H_{ij}^n .

For the nonrotating stars, C_0 and C_1 appear to be unchanged throughout the simulations. Thus, to determine $C_0(r)$ and $C_1(r)$ at each radius, a least-square fitting against the gauge-invariant variables is carried out in the time domain. For the fitting, all the data sets with $t - r_* \geq 0$ are used.

For the rotating stars, on the other hand, C_0 and, in particular, C_1 suddenly change at $t - r_* \sim 300M$. (The reason is not very clear.) Thus, these coefficients are separately

determined for $t - r_* \gtrsim 300M$ and $t - r_* \lesssim 300M$, carrying out the least-square fitting with two different data sets. Namely, we subtract a function of the form

$$\begin{cases} C_0(r) + C_1(r)t & \text{for } t \leq t_m(r), \\ C'_0(r) + C'_1(r)t & \text{for } t \geq t_m(r), \end{cases} \quad (39)$$

where $t_m(r)$ is a time $\sim 300M$ and satisfies the relation $C_0(r) + C_1(r)t_m(r) = C'_0(r) + C'_1(r)t_m(r)$ at each radius.

To validate that modified waveforms depend weakly on the subtraction method, the following alternative method is also adopted: According to Eq. (38), C_0 and C_1 for R_2^E are expressed by linear combinations of the functions r^4 , r^2 , r^{-1} , and r^{-3} . For a large value of the extraction radius L_e , we may expect that $C_0 \approx 0$ and $C_1 \propto r^4$ at the leading order. In this assumption, C may be computed as

$$C \approx \frac{r_2 R_2^E(r_2) - r_1 R_2^E(r_1)}{r_2^5 - r_1^5} L_e^5, \quad (40)$$

where r_1 and r_2 denote two different radii which is close to L_e . After the subtraction of the dominant part, it is found that a component of small magnitude associated with C_0 still remains. To eliminate this remaining nonwave part, we simply subtract a constant from the resulting waveform.

In addition to the least-square fitting method, we have also adopted this method and confirmed that the subtracted waveforms by this alternative method agree approximately with those in the least-square fitting (the wave phases agree well, and relative difference of the amplitude is within 10%). Thus, in the following, numerical results based on the subtraction using the least-square fitting are presented.

In Figs. 1(b) and 2(b), we display improved gravitational waveforms $rh_+/\sin^2\theta$ obtained after the nonwave components and the numerical errors are subtracted. It is found that the resulting wave amplitude and phase depend very weakly on the extracted radii for $t - r_* > 0$. This confirms that the extracted components are certainly gravitational waves.

For the rotating star, the amplitudes of the gravitational waveforms extracted at different radii are in slight disagreement each other. Figure 2(b) shows that the magnitude of the

difference is $\sim 10^{-3}$. This indicates that even in the improved waveforms, numerical errors of magnitude $\sim 10^{-3}$ still remain. The origin is likely to be a nonsystematic error such as spurious wave components.

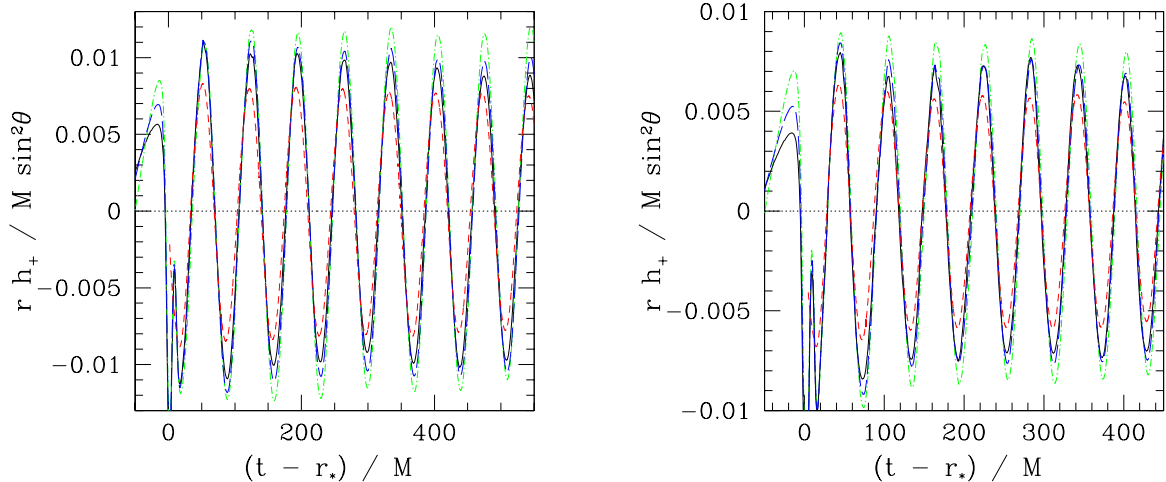
Besides quasiperiodic waves, a spike is visible at the beginning of the simulation (at $t \sim 10M$) in Figs. 1 and 2. We do not understand the origin of it exactly. The following is inference for the possible origin: At $t=0$, we rather crudely add a weakly nonlinear velocity perturbation to equilibrium states. Because of the weak nonlinearity, impulsive gravitational waves may be excited besides eigen oscillation modes of the equilibrium stars. Such impulsive gravitational waves seem to propagate at $t - r \sim 0$.

Before closing this subsection, we note the following: The magnitude of the numerical error associated with H_{ij}^n is not very large in three-dimensional simulations for binary neutron star merger [19] and oscillation of neutron stars [17], although it might be contained. We suspect that the excitation of such unphysical modes may be associated with the interpolation used in the Cartoon method. (In this paper, we simply adopt a second-order interpolation.) This suggests that there would be still a room to improve the interpolation scheme in our numerical implementation.

C. Gravitational waveforms

1. Nonrotating stars

Improved gravitational waveforms with $l = 2$ from axisymmetrically oscillating and nonrotating neutron stars for models S2 and S3 are displayed in Fig. 3. For both models, the simulations were performed with $N = 480$ (dotted-dashed curves), 600 (long-dashed curves), and 720 (solid curves). Gravitational waveforms evaluated by the quadrupole formula (dashed curves) are displayed together to illustrate its validity. The quadrupole formula was used in all the simulations and it is found that the gravitational waveforms depend very weakly on the value of N . Here, the numerical results for $N = 720$ are plotted.



(a) (b)
 FIG. 3. Gravitational waves with $l = 2$ from nonrotating neutron stars with axisymmetric oscillations (a) for models S2 (left) and (b) S3 (right). For both models, we show the results with $N = 480$ (dotted-dashed curve), 600 (long-dashed curve), and 720 (solid curve). The dashed curves denote the corresponding gravitational waveforms by the quadrupole formula. Here, the gravitational waveforms are extracted at $L_e \sim 0.9L$. Note that the behavior of the raw data is very similar to that in Fig. 1, i.e., with the increase of L_e (with the increase of N for a fixed grid spacing), the amplitude of the drift is larger.

Figure 3 indicates that one oscillation mode is dominantly excited. As a result, the waveforms are well-approximated by a simple sine curve. Indeed, the Fourier spectra of $rh_+^{\text{quad}}/\sin^2\theta$ possess one sharp peak, and the oscillation periods are ≈ 0.84 , 0.84 , and 0.85 in units of $2\pi\sqrt{R^3/M}$ for models S1, S2, and S3, respectively [†]. Thus, irrespective of compactness of the neutron stars, the oscillation period is $\approx 0.85 \times 2\pi\sqrt{R^3/M}$. This implies that the oscillation is associated with the fundamental quadrupole mode, since the

[†]In [15], a three-dimensional simulation for an oscillating and nonrotating star which is almost the same as model S1 was performed. They computed approximate gravitational waveforms in a near zone ($\lambda/L \approx 0.12$) and derived the period for the fundamental quadrupole mode as $0.83\pi\sqrt{R^3/M}$. This value agrees with ours in $\sim 1\%$ error.

coefficient (≈ 0.85) depends very weakly on the compactness of the neutron stars for a given equation of state [26].

From Eq. (14), the luminosity of gravitational radiation as a function of time is computed. Since the luminosity also varies in a periodic manner, we define an averaged energy flux according to

$$\left\langle \frac{dE}{dt} \right\rangle \equiv \frac{1}{P_{\text{osc}}} \int_{t_0}^{t_0+P_{\text{osc}}} \frac{dE}{dt} dt, \quad (41)$$

where t_0 is a constant. For models S1–S3, the averaged luminosity is $\sim 6 \times 10^{-8}$ (in units of $G^{-1}c^5$). Therefore, the energy dissipated in one oscillation period is much smaller than the total mass energy of the system and the radiation reaction timescale is much longer than the oscillation period.

Figures 1 and 3 indicate that (i) the wave length is independent of L and L_e , (ii) the amplitude of gravitational waves is overestimated for the smaller values of L and L_e , and (iii) the amplitude for model S3 approximately converges to an asymptotic value for $N \gtrsim 600$ within $\sim 10\%$ error. These facts suggest that for $L_e \gtrsim \lambda$ (see Table II), convergent gravitational waveforms within 10% error can be computed. On the other hand, if the outer boundaries are located in a near zone with $L < \lambda$, the amplitude of gravitational waves is overestimated: For $L \approx 2\lambda/3$, it is overestimated by a factor of $\sim 20\%$. This result is consistent with that in our previous study for gravitational waves from binary neutron stars in quasiequilibrium circular orbits [28].

The quadrupole formula yields well-approximated gravitational waveforms besides a systematic underestimation of the wave amplitude. For models S2 and S3, the asymptotic amplitudes of A_2/M are about 0.010 and 0.007, respectively. On the other hand, according to the quadrupole formula, they are about 0.008 and 0.0055. Thus, the underestimation factor is $\sim 20\%$. If it is due to the first post Newtonian correction, the factor should be proportional to the compactness of neutron stars $M/R(= GM/Rc^2)$ or $v^2(= v^2/c^2)$ where v denotes typical magnitude of the oscillation velocity. To determine which the dominant component is, we performed a simulation reducing the magnitude of the velocity perturba-

tion initially given (i.e., reducing the magnitude of V) and found that the wave amplitude is underestimated by $\sim 20\%$ irrespective of the magnitude of V . Therefore, we conclude that the underestimation factor is proportional to the magnitude of M/R in the present case.

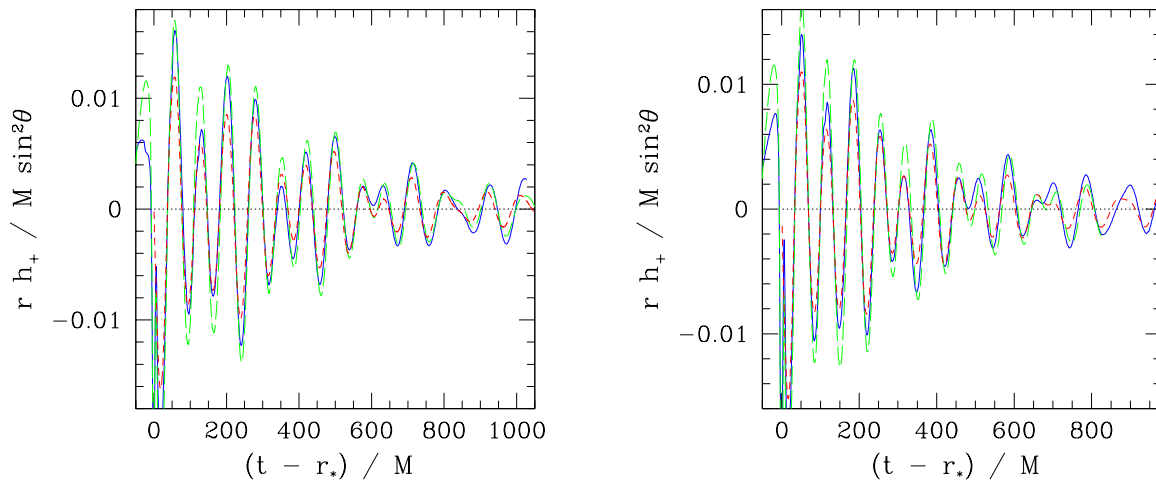
Although the wave amplitude is underestimated, the wave phase is computed accurately by the quadrupole formula. The most important element in detection of gravitational waves using matched filtering techniques is to a priori know the phase of gravitational waves. From this point of view, the quadrupole formula is a useful tool for computation of gravitational waveforms.

2. Rotating stars

In Fig. 4, gravitational waveforms with $l = 2$ from oscillating and rapidly rotating neutron stars for models R2 and R3 are displayed. For these simulations, velocity perturbations are added initially without changing other quantities. The numerical results are shown for $N = 480$ (long-dashed curve) and 720 (solid curve). For $N = 480$ and 720, the gauge-invariant variables are extracted at $\approx 2\lambda/3$ and λ , respectively. The waveforms computed by the quadrupole formula (dashed curves) are displayed together.

In contrast to those from oscillating and nonrotating neutron stars, the gravitational waveforms are not of simple sine curve. There are two main reasons. One is the following: In the nonrotating case, the restoring forces against a compression for ϖ and z directions are of identical magnitude and, hence, the oscillation periods of two directions agree. For the rotating stars, on the other hand, the two restoring forces are not of identical magnitude and, therefore, the oscillation periods of two directions do not agree. Due to this fact, the waveforms are composed of more than two oscillation modes.

The other reason is that gravitational waves are emitted due to a quasiradial motion in the case of rotating neutron stars in contrast to nonrotating neutron stars. In particular, we here choose rapidly rotating neutron stars and, therefore, the wave amplitude can be as larger as than for the quadrupole oscillations.



R2 R3
 FIG. 4. Gravitational waves with $l = 2$ from rotating neutron stars R2 (left) and R3 (right) with $N = 480$ (long-dashed curve) and 720 (solid curve). The dashed curves denote the results by the quadrupole formula.

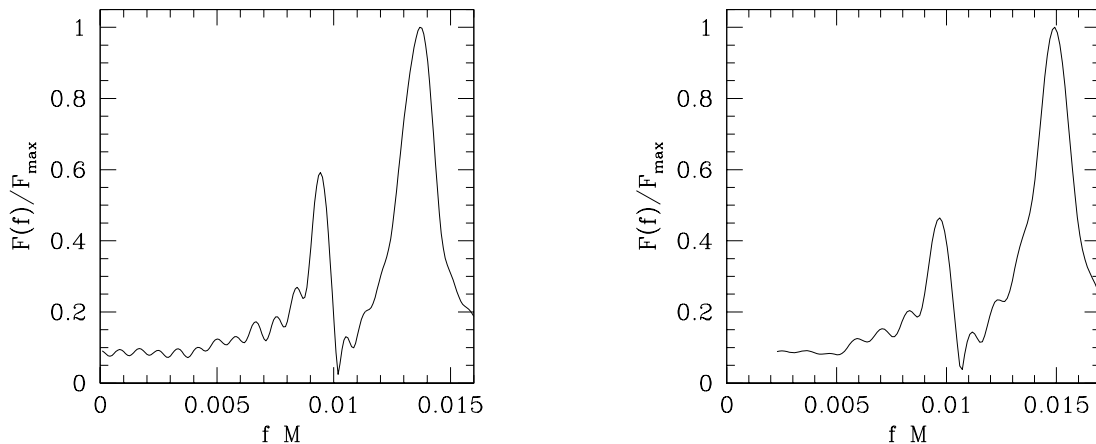
To clarify what oscillation modes are relevant, the Fourier spectrum $F(f)$ for models R2 and R3 are displayed in Fig. 5. This shows that there are two characteristic peaks in the spectrum. The oscillation periods defined by $1/f_{\text{peak}}$ where f_{peak} is the frequency of the peaks in the Fourier spectrum are listed in Tables I and III.

For models R1–R3, the oscillation period of the larger frequency is

$$P_{\text{osc}} \approx 0.5 \times 2\pi \sqrt{\frac{R^3}{M}}, \quad (42)$$

where R is the equatorial circumferential radius. The coefficient (≈ 0.5) depends very weakly on the compactness of the neutron star. This indicates that the oscillation mode is the fundamental *quadrupole* mode.

The frequency of the other peak is smaller than that of the fundamental quadrupole mode. This peak is likely to be associated with the fundamental *quasiradial* oscillation mode (p_1 mode). To confirm this prediction, we performed the Fourier analysis to the time sequence of the central density and found that the characteristic oscillation period indeed coincides with that of the second peak (see Table III). Furthermore, it agrees with



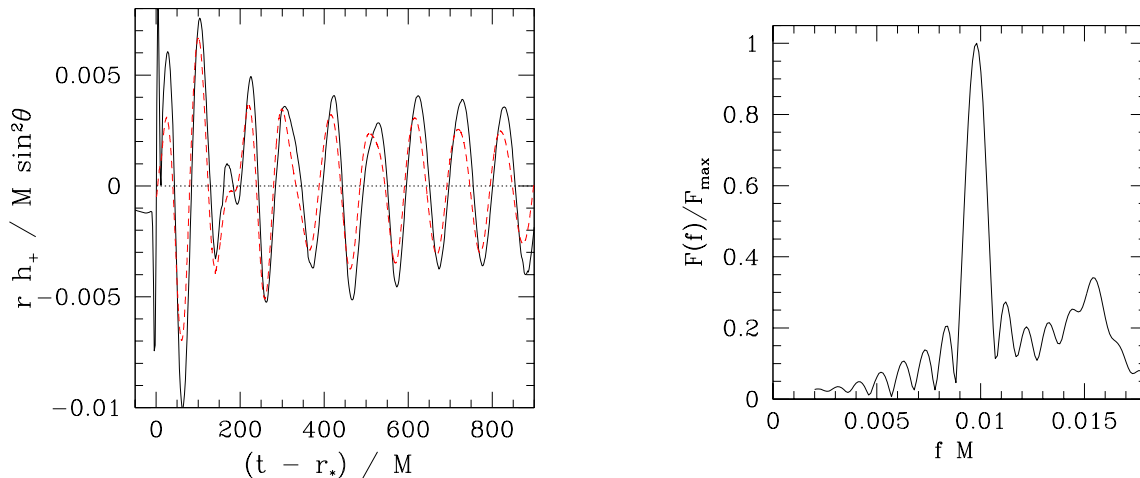
R2 R3
 FIG. 5. The Fourier spectrum of gravitational waveforms for models R2 (left) and R3 (right). The spectrum is normalized by the maximum value, and the frequency f is shown in units of M^{-1} . The peaks of the smaller and larger frequencies indicate the quasiradial and quadrupole modes, respectively.

the characteristic frequency for quasiradially oscillating neutron stars presented in [12]. All these facts confirm our prediction.

The Fourier spectra indicate that gravitational waves from axisymmetric global oscillations of rigidly rotating stars are composed of two dominant modes. To confirm this conjecture, we performed simulations initiated from another initial condition in which the pressure is uniformly depleted but the velocity field is unperturbed. To uniformly deplete the pressure, K is decreased by 20% at $t = 0$. In Fig. 6, we display (a) the gravitational waveform and (b) the Fourier spectrum for model R1 for this simulation. Figure 6 (b) shows that two modes, the fundamental quadrupole and quasiradial ones, are dominant again. This result justifies our conjecture. In contrast to the cases in which the nonspherical velocity perturbation is added, the mode with lower frequency, i.e., the quasiradial mode, is dominant. This is because the matter motion is almost quasiradial.

In the collapse of massive rotating stellar core, a protoneutron star will be formed. If the progenitor star is not rapidly rotating and its degree of differential rotation is not high,

the protoneutron star relaxes to a nearly quasistationary state soon after the collapse (e.g., [1]). At the formation of a rotating protoneutron star in a nearly quasistationary state, nonspherical oscillations are excited by the quasiradial infall. Because of the nonspherical nature, gravitational waves are emitted [1]. As illustrated above, in such oscillating neutron stars in a nearly quasistationary state, two dominant modes (quasiradial and quadrupole modes) may be excited. If the collapse is quasiradial, the quasiradial mode will be the main component. On the other hand, if the nonspherical quadrupole oscillation of high amplitude is excited, the quadrupole mode will be dominant.



(a) (b)
 FIG. 6. (a) Gravitational waves with $l = 2$ from rotating neutron stars R1 in a quasiradial oscillation with $N = 480$ (solid curve). The dashed curves denote the results by the quadrupole formula. (b) The Fourier spectrum of gravitational waves. The spectrum is normalized by the maximum value, and the frequency f is shown in units of M^{-1} . The peaks of the smaller and larger frequencies indicate the quasiradial and quadrupole modes, respectively. In this case, the quasiradial mode is dominant (compare with Fig. 5).

As Fig. 4 shows, the wave amplitude decreases with time in the early phase ($t - r_* \lesssim 500M$), and then relaxes to a small value. On the other hand, the amplitude does not decrease in Fig. 6. This indicates that the amplitude of the quadrupole oscillation decreases with time to a small value, while the quasiradial oscillation does not. As mentioned above,

the oscillation frequencies for z and ϖ directions are not identical for the quadrupole oscillation of rotating stars. As a result, shocks may be formed at a collision of compression waves in the two different oscillation directions. Repeating this process, the quadrupole oscillation may be gradually damped. On the other hand, there is no process that damps quasiradial mode quickly. Thus, it is reasonable to expect that the quasiradial mode eventually dominates in the oscillating and rotating stars.

Using Eq. (14), the luminosity is computed. It is found that until $t \sim 1000M$, the total radiated energy is computed as $\sim 5 \times 10^{-5}M$, which is much smaller than the total mass energy of the system. Therefore, the damping timescale of the wave amplitude due to gravitational waves is much longer than the oscillation and rotation periods.

As in the nonrotating case, approximate gravitational waveforms were computed using the quadrupole formula. Figures 4 and 6 indicate that the waveforms agree with those computed by the gauge-invariant method, besides a systematic underestimation of the amplitude. The underestimation factor is of order M/R as in the nonrotating cases. In the case of rotating stars, a modulation of the wave amplitude is outstanding. Using the quadrupole formula, however, such modulation can be well computed. As mentioned in IV C 1, the most important element in detection of gravitational waves using matched filtering techniques is to a priori know the phase and modulation of gravitational waves. The results here indicates that they are computed well in the quadrupole formula. Therefore, for computation of gravitational waves in rotating stellar core collapse to a protoneutron star, the quadrupole formula may be a useful tool.

V. SUMMARY AND DISCUSSION

We have studied gravitational waves from axisymmetrically oscillating neutron stars adopting the gauge-invariant wave extraction method as well as the quadrupole formula. It is found that several types of the nonwave components such as the stationary parts of metric and numerical errors are contained in the gauge-invariant variables. The numerical

	$P_{\text{osc}}/(2\pi R^{3/2} M^{-1/2})$ (for central density)	$P_{\text{osc}}/(2\pi R^{3/2} M^{-1/2})$ (for gravitational waves)	Ref. [12]
R1	0.66	0.66	0.66
R2	0.69	0.70	—
R3	0.76	0.76	0.76

TABLE III. $P_{\text{osc}}/(2\pi R^{3/2} M^{-1/2})$ for the fundamental quasi-radial mode calculated from the evolution of the central density and gravitational waveforms. The last column shows the results obtained from simulations of the quasiradial oscillation.

errors are generated due to an approximate treatment for the outer boundary conditions. We illustrate a method to subtract the dominant components of the numerical errors and demonstrate it possible to extract gravitational waves even from such noisy data sets with a residual of magnitude $\sim 10^{-3}$.

The gravitational waveforms computed in the quadrupole formula agree well with those obtained from the gauge-invariant technique besides a systematic underestimation of the amplitude by $\sim 20\%$. An important point is that the evolution of the wave phase and the modulation of the amplitude are computed with a good accuracy. This indicates that for a study of gravitational waveforms from rotating stellar core collapse to a protoneutron star, the quadrupole formula will be a useful tool in fully relativistic simulations. It should be also addressed that the result in this paper supports the treatment in [1] in which gravitational waveforms are computed using a quadrupole formula in approximate general relativistic simulations.

The gauge-invariant variables are extracted for various values of extraction radii. It is found that to extract gravitational waves within $\sim 10\%$ error, the extraction radius has to be larger than $\sim 90\%$ of the gravitational wave length. If the outer boundaries are located in the near zone with $L < \lambda$, the amplitude of gravitational waves is overestimated: For $L \approx 2\lambda/3$, it is overestimated by $\sim 20\%$. For $L < 2\lambda/3$, the factor of the overestimation is

even larger.

In the present work, the amplitude of gravitational waves in a local wave zone is much larger than that of systematic numerical errors. This fact enables to subtract them from the gauge-invariant variables accurately. If the magnitude of the errors is much larger than that of the amplitude of gravitational waves, however, it would not be possible to carry out an accurate subtraction. For example, in rotating stellar core collapse, the amplitude of gravitational waves in the local wave zone at $r \sim \lambda$ is at most $\sim 10^{-5}$ according to gravitational waveforms calculated by a quadrupole formula [1]. To extract gravitational waves of such small amplitude, it is necessary to reduce the magnitude of the numerical errors. To achieve that, we need to impose more accurate outer boundary conditions. Developing such conditions is crucial in computing gravitational waves of small amplitude of $O(10^{-5})$ from raw data sets of metric.

Another possible method for computing accurate gravitational waves of small amplitude is to adopt a quadrupole formula taking into account higher-order post Newtonian terms. As indicated in this paper, the simple quadrupole formula underestimates the amplitude of gravitational waves by $O(M/R)$. In rotating stellar core collapse, the error in the amplitude will be $\sim 10\%$. To compute the amplitude within $\sim 1\%$ error, we should take into account higher general relativistic corrections. In quadrupole formulas with the higher post Newtonian corrections (as derived in [29]), it may be possible to obtain gravitational waveforms within 1% error. Such formulas will be useful to extract gravitational waves of small amplitude from rotating stellar core collapses and from oscillating neutron stars.

In addition to the study for gravitational wave extraction, oscillation modes of rotating neutron stars are analyzed. It is found that two modes (the fundamental quadrupole and quasiradial modes) are dominantly excited due to the global oscillation. The frequency of the quadrupole mode is proportional to $\sqrt{GM/R^3}$, and is higher than that of the quasiradial one for the typical values of mass and radius of neutron stars. It is shown that the amplitude of the quadrupole mode decreases with time due to an incoherent nature of the oscillation, but that of the quasiradial mode is not damped quickly, hence being the dominant mode after

several dynamical timescales. We expect that in rotating stellar core collapse to a protoneutron star in a nearly quasistationary state, these two modes may be the main components in the burst phase of gravitational waves. The quadrupole mode will be damped within a few dynamical timescales and subsequently the quasiradial mode will be the dominant component to be longterm quasiperiodic waves.

Acknowledgments

Numerical computations were carried out on the FACOM VPP5000 machine in the data processing center of National Astronomical Observatory of Japan. This work is in part supported by Japanese Monbu-Kagakusho Grant (Nos. 13740143, 14047207, 15037204, and 15740142).

APPENDIX A: SOLUTIONS FOR THE TENSOR LAPLACE EQUATION

Here, we describe solutions for the tensor Laplace equations in spherical polar coordinates as

$$\Delta_f h_{ab} = 0. \tag{A1}$$

h_{ab} is expanded by tensor harmonic functions as

$$h_{ab} = \sum_l \begin{pmatrix} A_l Y_{l0} & r B_l Y_{l0,\theta} & 0 \\ * & r^2 (K_l Y_{l0} + G_l W_{l0}) & 0 \\ * & * & r^2 \sin^2 \theta (K_l Y_{l0} - G_l W_{l0}) \end{pmatrix} + \begin{pmatrix} 0 & 0 & r C_l \partial_\theta Y_{l0} \sin \theta \\ * & 0 & -r^2 D_l W_{l0} \sin \theta \\ * & * & 0 \end{pmatrix}, \tag{A2}$$

where A_l , B_l , C_l , D_l , G_l , and K_l are functions of r . With the above expansion, the components of the Laplace equation are written as

$$\begin{aligned}
\Delta_f h_{rr} &= \sum_l \left[A_l'' + \frac{2}{r} A_l' - \frac{\lambda_l + 4}{r^2} A_l + \frac{4}{r^2} K_l + \frac{4\lambda_l}{r^2} B_l \right] Y_{l0} = 0, \\
\Delta_f h_{r\theta} &= r \sum_l \left[B_l'' + \frac{2}{r} B_l' - \frac{\lambda_l + 4}{r^2} B_l + \frac{2}{r^2} A_l - \frac{2}{r^2} K_l + \frac{2\lambda_l - 4}{r^2} F_l \right] \partial_\theta Y_{l0} = 0, \\
\Delta_f h_{r\varphi} &= r \sum_l \left[C_l'' + \frac{2}{r} C_l' - \frac{\lambda_l + 4}{r^2} C_l + \frac{-2\lambda_l + 4}{r^2} D_l \right] \frac{\partial_\varphi Y_{l0}}{\sin \theta} = 0, \\
\frac{\Delta_f h_{\theta\varphi}}{r^2} &= \sum_l \left[D_l'' + \frac{2}{r} D_l' - \frac{\lambda_l - 2}{r^2} D_l - \frac{2}{r^2} C_l \right] \sin \theta W_{l0} = 0, \\
\frac{\Delta_f h_{\theta\theta}}{r^2} &= \sum_l \left[\left(K_l'' + \frac{2}{r} K_l' - \frac{\lambda_l + 2}{r^2} K_l + \frac{2}{r^2} A_l - \frac{2\lambda_l}{r^2} B_l \right) Y_{l0} + \left(F_l'' + \frac{2}{r} F_l' - \frac{\lambda_l - 2}{r^2} F_l + \frac{2}{r^2} B_l \right) W_{l0} \right] \\
&\equiv \sum_l \left(H_l^k Y_{l0} + H_l^f W_{l0} \right) = 0, \\
\frac{\Delta_f h_{\varphi\varphi}}{r^2 \sin^2 \theta} &= \sum_l \left(-H_l^k Y_{l0} - H_l^f W_{l0} \right) = 0, \tag{A3}
\end{aligned}$$

where $\lambda_l = l(l+1)$ and $'$ denotes d/dr .

Setting $A_l = \bar{A}_l r^n$, $B_l = \bar{B}_l r^n$, $K_l = \bar{K}_l r^n$, and $F_l = \bar{F}_l r^n$ where $\bar{A}_l \sim \bar{F}_l$ are constants, simultaneous equations for the even-parity modes are derived as

$$\begin{pmatrix} x-4 & 4\lambda_l & 4 & 0 \\ 2 & x-4 & -2 & 2\lambda_l-4 \\ 2 & -2\lambda_l & x-2 & 0 \\ 0 & 2 & 0 & x+2 \end{pmatrix} \begin{pmatrix} \bar{A}_l \\ \bar{B}_l \\ \bar{K}_l \\ \bar{F}_l \end{pmatrix} = 0, \tag{A4}$$

where $x = n(n+1) - \lambda_l$. For the existence of the solutions, the determinant of the matrix should be zero. Then, an algebraic equation for n is derived, and the solutions are $n = l \pm 2$, l , $-l \pm 1$ and $-l - 3$. The relations among $\bar{A}_l \sim \bar{F}_l$ are easily obtained for each value of n . It is also easy to check that the solutions with $n = l - 2$ and $-l - 3$ are written in the form $V_{i|j} + V_{j|i}$ using a vector V_i of even-parity.

From the same procedure, the solutions for the odd-parity mode are written as $C_l = \bar{C}_l r^n$ and $D_l = \bar{D}_l r^n$ where $n = l \pm 1$, $-l$ and $-l - 2$, and \bar{C}_l and \bar{D}_l are constants. In this case, the solutions with $n = l - 1$ and $-l - 2$ are written as $V_{i|j} + V_{j|i}$ using a vector V_i of odd-parity.

REFERENCES

- [1] H. Dimmelmeier, J. A. Font and E. Müller, *Astron. Astrophys.* **388**, 917 (2002); **393**, 523 (2002).
- [2] F. Siebel, J. A. Font, E. Müller and P. Papadopoulos, *Phys. Rev. D* **67**, 124018 (2003).
- [3] L. S. Finn and C. R. Evans, *Astrophys. J.* **351**, 588 (1990).
- [4] R. Mönchmeyer, G. Schäfer, E. Müller and R. Kates, *Astron. and Astrophys.* **246**, 417 (1991); E. Müller and H.-T. Janka, *Astron. Astrophys.* **103**, 358 (1997).
- [5] S. Bonazzola and J.-A. Marck, *Astron. Astrophys.* **267**, 623 (1993).
- [6] S. Yamada and K. Sato, *Astrophys. J.* **434**, 268 (1994); **450**, 245 (1995); K. Kotake, S. Yamada, and K. Sato, *Phys. Rev. D* **68**, 044023 (2003).
- [7] T. Zwerger and E. Müller, *Astron. Astrophys.* **320**, 209 (1997); M. Rampp, E. Mühle and M. Ruffert, *Astron. Astrophys.* **332**, 969 (1998).
- [8] C. Fryer and A. Heger, *Astrophys. J.* **541**, 1033 (2000); C. Fryer, D. E. Holz and A. Heger, *Astrophys. J.* **565**, 430 (2002).
- [9] C. D. Ott, A. Burrows, E. Livne, and R. Walder, *Astrophys. J.* **600**, 834 (2004).
- [10] A. M. Abrahams and C. R. Evans, *Phys. Rev. D* **37**, 318 (1988); **42**, 2585 (1990).
- [11] F. Siebel, J. A. Font, E. Müller and P. Papadopoulos, *Phys. Rev. D* **65**, 064038 (2002).
- [12] M. Shibata, *Phys. Rev. D* **67**, 024033 (2003).
- [13] M. Alcubierre, S. Brandt, B. Brügmann, D. Holz, E. Seidel, R. Takahashi and J. Thornburg, *Int. J. Mod. Phys. D* **10**, 273 (2001).
- [14] J. A. Font, *Living Review Relativity* **3**, 2, 2000 <http://www.livingreviews.org/Articles/Volume2/2000-2font>; F. Banyuls, J. A. Font, J.-Ma. Ibáñez, J. M. Martí, and J. A. Miralles, *Astrophys. J.* **476**,

- 221 (1997).
- [15] J. A. Font, T. Goodale, S. Iyer, M. Miller, L. Rezzolla, E. Seidel, N. Stergioulas, W. M. Suen and M. Tobias, Phys. Rev. D **65**, 084024 (2002).
- [16] M. Shibata, Prog. Theor. Phys. **101**, 1199 (1999); Prog. Theor. Phys. **104**, 325 (2000).
- [17] M. Shibata, Phys. Rev. D **60**, 104052 (1999).
- [18] M. Shibata, T. W. Baumgarte and S. L. Shapiro, Phys. Rev. D **61**, 044012 (2000); Astrophys. J. **542**, 453 (2000).
- [19] M. Shibata and K. Uryū, Phys. Rev. D **61**, 064001 (2000): Prog. Theor. Phys. **107**, 265 (2002).
- [20] In [16,18,19] and this paper, we adopt a formulation slight modified from the original version presented in the following reference: M. Shibata and T. Nakamura, Phys. Rev. D **52**, 5428 (1995). See also T. Nakamura, K. Oohara, and Y. Kojima, Prog. Theor. Phys. Suppl. **90**, 1 (1987).
- [21] M. Shibata, Astrophys. J. **595**, 992 (2003).
- [22] V. Moncrief, Ann. of Phys. **88**, 323 (1974)
- [23] A. Abrahams, D. Bernstein, D. Hobill, E. Seidel and L. Smarr, Phys. Rev. D **45**, 3544 (1992).
- [24] S. A. Teukolsky, Phys. Rev. D **26**, 745 (1982).
- [25] G. Cook, S. L. Shapiro, and S. A. Teukolsky, Astrophys. J. **422**, 227 (1994).
- [26] Y. Kojima, Prog. Theor. Phys. **77**, 297 (1987).
- [27] T. Nakamura, Prog. Theor. Phys. **72**, 746 (1984).
- [28] M. Shibata and K. Uryū, Phys. Rev. D **64**, 104017 (2001).

[29] L. Blanchet, T. Damour and G. Schäfer, *Mon. Not. R. astr. Soc.* **242**, 289 (1990).